

modes. Structural differences among polyelectrolyte coatings are anticipated to produce quantitative variations in the relative importance of the two phases in charge propagation and in the importance of coupling between the propagation pathways in each phase. The rates of all three processes appear to be remarkably high with PLL coatings in which $\text{Fe}^{\text{III/II}}(\text{edta})$ anions are incorporated. The highly swollen, flexible structure provided by the PLL coatings appears to be the common basis for the high rate of all three processes.

The use of variations (if any) in reactant diffusion coefficients to distinguish between ion hopping and electron hopping as the mechanism of charge transport within the Donnan domains was also demonstrated. The form of the general equation for the steady-state electrochemical behavior of redox self-exchange reactions at polyelectrolyte-coated electrodes (eq 9) requires revision in the previously suggested¹ formula for estimating electron-exchange rate constants.

Although the two-phase model of Figure 1 has been tested for the case of $\text{Fe}^{\text{III/II}}(\text{edta})$ in PLL, we believe the essential features of the model and the consequences to which they lead should be generally applicable to polyelectrolyte-coated electrodes.

Acknowledgment. This work was supported in the U.S.A. by the National Science Foundation and the U.S. Army Research Office and in France by the CNRS (Equipe de Recherche Associée 309 "Electrochimie Moleculaire", ATP, "Epargnes d'Énergie et de Matières Premières"). We are grateful to Claude P. Andrieux, Daniel Buttry, and Takeo Ohsaka for numerous helpful discussions and to the North Atlantic Treaty Organization for a Collaborative Research Grant.

Registry No. $\text{Fe}^{\text{II}}(\text{edta})^-$, 15275-07-7; $\text{Fe}^{\text{III}}(\text{edta})^{2-}$, 15651-72-6; $\text{Fe}^{\text{III}}(\text{Heedta})$, 17084-02-5; $[\text{Co}(\text{C}_2\text{O}_4)_2(\text{NH}_3)_2]^-$, 39141-87-2; $\text{Zr}^{\text{II}}(\text{edta})^{2-}$, 12519-36-7; CH_3COONa , 127-09-3; PLL, 26588-20-5; graphite, 7782-42-5.

Transient Spontaneous Raman Study of Photoionization Kinetics at the Hydrocarbon/Water Interface in Micellar Solutions

S. M. Beck and L. E. Brus*

Contribution from Bell Laboratories, Murray Hill, New Jersey 07974. Received June 8, 1982

Abstract: Transient spontaneous Raman spectroscopy (416 nm) has been used to observe the kinetics of TMB^+ and TMB^{2+} ions following photoionization of tetramethylbenzidine (TMB) in aqueous micellar solutions. The ground-state TMB $\text{p}K_a$ values are shifted by micellar solubilization in the directions predicted by calculated surface pH values. In SDS micelles, the TMB^+ ion initially produced is stabilized by negative surface groups. No time evolution of the TMB^+ Raman spectrum occurs, and bimolecular ion reactions are not observed. However, in CTAB micelles, TMB^+ is destabilized by positive surface groups. The TMB^+ Raman spectrum evolves on the 10^{-6} -s time scale, suggesting that the ion has moved into the Stern layer and is asymmetrically solvated. On the 10^{-4} -s time scale, TMB^{2+} appears from disproportionation of two TMB^+ ions. Positive spectral identifications are facilitated by comparison with spectra obtained by chemical oxidation in various environments.

Introduction

Condensed-phase chemical reactions are often strongly dependent upon solvation. In enzymes and membranes, a coordinated local arrangement of solvating molecules can completely control a reaction in the catalytic sense. These systems are often microscopically heterogeneous, in that a region of hydrophobic character exists within a few ångströms of a region of hydrophilic character. Aqueous micellar solutions provide a simple example exhibiting similar structural features. A hydrocarbon-like micellar interior, of perhaps 40-Å diameter, is separated from an aqueous phase by an ionic double-layer boundary region. A static potential gradient exists across the boundary region. This gradient is of opposite sign in cationic and anionic micelles. Recent experiments have utilized such systems to permanently separate charge following photoionization, and to preferentially stabilize organic cations in the interior of anionic micelles.¹

A given molecular species can be preferentially stabilized in the interior of a micelle, on its boundary (Stern layer), or in the aqueous phase, depending upon the balance of hydrophobic and hydrophilic interactions and the sign of the surface potential. Aromatic neutral molecules often dissolve in the hydrocarbon-like micelle interior. A pulse of light can photoionize such species, with the ejected electron becoming solvated in the aqueous phase. The resulting molecular anion might be preferentially stabilized

in the boundary region or the aqueous phase. In some systems, then, an initial photoionizing pulse may create a cation which subsequently moves out from the micelle interior. The ejected electron could be captured by a preexisting different cation in the boundary double layer region, with the result that the reduced species moves in toward the micellar interior. Thus, in time-resolved, pump-probe spectroscopic experiments, one might monitor the motion of transient species across the double-layer region.

Transient electronic absorption offers excellent detection sensitivity, yet provides little structural information because of the diffuse nature of the spectra. Transient spontaneous Raman spectroscopy, yielding direct vibrational information, offers a number of advantages in the study of chemical kinetics. This application has been clearly demonstrated in previous examples of homogeneous solution reactions.² In this paper we apply Raman spectroscopy to the study of molecular motion and reaction in micellar solutions. We have previously noted the feasibility of hydrocarbon/aqueous interface kinetics studies, and the enhanced detection sensitivity of transient Raman experiments, in micellar solutions.³ The essential question is the degree to which the spectra are sensitive to the nature of the local environment. A similar question has been addressed in hemoglobin studies,

(1) (a) N. J. Turro, M. Grätzel, and A. M. Braun, *Angew. Chem., Int. Ed. Engl.*, **19**, 675 (1980); (b) J. K. Thomas, *Acc. Chem. Res.*, **10**, 133 (1977).

(2) (a) S. M. Beck and L. E. Brus, *J. Chem. Phys.*, **75**, 4934 (1981); (b) R. F. Dollinger and W. F. Woodruff, *J. Am. Chem. Soc.*, **101**, 4391 (1979); (c) R. Wilbrant, P. Paqsberg, K. B. Handson, and K. V. Weisberg, *Chem. Phys. Lett.*, **36**, 76 (1975).

(3) S. M. Beck and L. E. Brus, *J. Chem. Phys.*, **75**, 1031 (1981).

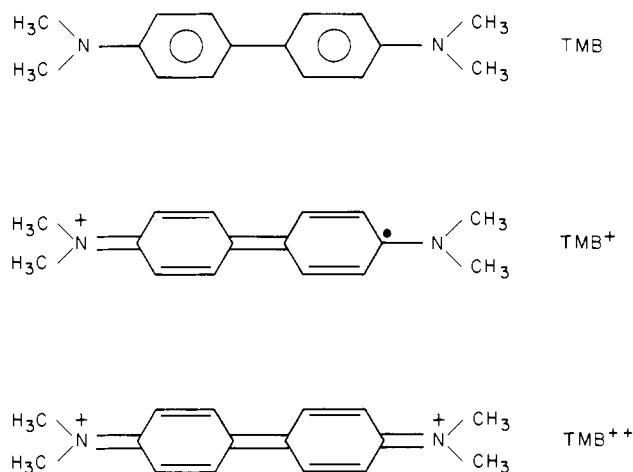


Figure 1. Chemical structures discussed in the text.

where subtle shape changes of heme ring Raman transitions have been correlated with changes in nearby protein structure.⁴

Tetramethylbenzidine (TMB in Figure 1) has a low gas-phase ionization potential (6.1–6.8 eV)⁵ and undergoes efficient photoionization in solution. TMB is hydrophobic and dissolves in the hydrocarbon-like interior of the micelle. Anionic surfactants, such as sodium dodecyl sulfate (SDS), lower the ionization potential significantly by strongly solvating the cation with negative sulfate groups.⁶ A single near-UV photon, resonant with the S₁ state of TMB, is capable of ionizing the molecule in SDS with high efficiency.⁶ In cationic micelles, such as cetyltrimethylammonium bromide (CTAB), the triplet is predominately created by single photon absorption; however, at higher fluxes a sequential two-photon process can cause efficient photoionization.⁶

It has been known for years that both TMB⁺ and TMB²⁺ can be produced in polar organic solvents by photolysis or chemical oxidation.⁷ The absorption spectra of both ions are well characterized,^{6,7} consisting of strong absorption in the region 500 to 400 nm. TMB itself absorbs in the ultraviolet near 300 nm.

Irradiation in the region 530–400 nm produces strong pre-resonance and resonance Raman scattering in both ions, and recently a report of the steady-state resonance Raman (RR) spectrum of TMB⁺ in an ethanol glass at 77 K appeared.⁸ No Raman spectrum of TMB²⁺ to our knowledge has been reported.

In the present experiment, using RR spectroscopy, we examine the processes of photoassisted electron transfer and molecular motion across a micellar double layer. We begin with the effect of micellar environment on TMB protonation behavior and pK_a values. We then describe the simple photoionization behavior observed in SDS micelles where TMB⁺ is *stabilized* inside the micelle, and the complex behavior observed in CTAB micelles where TMB⁺ is *destabilized* inside the micelle. Finally we describe capture of the photoejected electron by methylviologen ion (MV²⁺) in the aqueous phase.

Experimental Section

Our experimental method has been detailed elsewhere,^{2a} and therefore only a brief account is now given. Two Q-switched Nd/YAG lasers (10 ns fwhm), independently fired, generate pump and probe optical pulses. The pump laser is either tripled to 355 nm or quadrupled to 266 nm. The

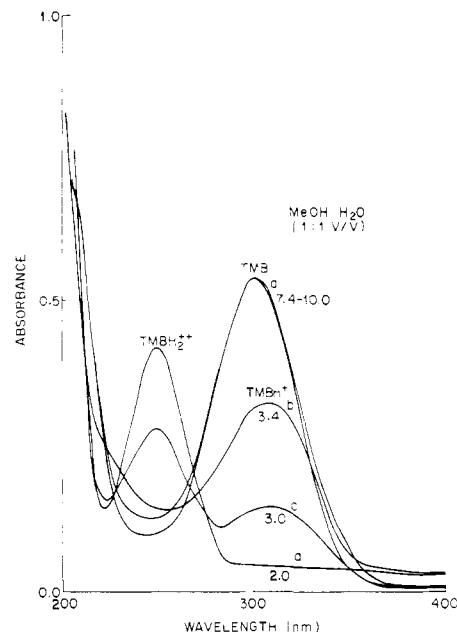


Figure 2. Absorption spectra of 10⁻³ M TMB in a 1:1 methanol/water mixture as a function of pH.

Table I

solvent	pK _{a1}	pK _{a2}
MeOH/H ₂ O	4.0	3.1
SDS	6.0	4.2
CTAB	2.8	

probe laser is tripled and then Raman shifted in H₂ to 416 nm. The two laser beams are spatially superimposed and brought to an approximate line focus in a flowing liquid stream. Transient species created by pump-pulse photolysis have their Raman spectrum generated by the probe pulse after some variable time, Δt. The Raman scattering is detected by a gated, intensified Reticon, and extensive signal averaging is employed to increase the signal to noise. This technique of pulsed excitation coupled with multichannel optical detection has been pioneered by Bridoux and Delhaye.⁹ Absorption spectra were obtained on a standard Cary 15 spectrometer.

All surfactants were used without purification in 0.2 M aqueous air-saturated solutions. The pH of the micellar solutions was adjusted by adding a few drops of ~1 M HCl or NaOH. TMB (Aldrich) was dissolved in micellar solutions by sonication and subsequent stirring. The concentration of TMB was monitored via absorption spectroscopy. A 10⁻³ M solution in SDS and CTAB micelles corresponds to an average occupation number of 0.2–0.4; that is, micelles predominately contain either no TMB or only one TMB molecule each.

Our ultraviolet photolyzing fluences per pulse are at least an order of magnitude higher than typically employed in transient absorption spectroscopy. This increase is necessary to compensate for the lower detection sensitivity of Raman spectroscopy as compared with absorption spectroscopy. Experimentally we observe in CTAB and SDS micellar solutions that the TMB⁺ Raman signals are of comparable magnitude and saturate with increasing 355-nm fluence. In both solutions we are ionizing a large fraction of the TMB molecules, yielding TMB⁺ concentrations near 10⁻³ M.

Results

1. Environmental Effect on TMB Protonation Equilibria. In order to correctly interpret the transient Raman data, it is necessary to establish the nature and physical location of TMB in solution before photoionization. This can be aided by analysis of electronic absorption spectra as a function of solvent and pH. As the spectra show interesting shifts in pK_a values as a function of local environment, we discuss these results in some detail.

Figure 2 shows the absorption spectra of a methanol and water (1:1 v/v) 10⁻³ M TMB solution as a function of pH. Three

(4) (a) J. A. Shelnut, D. L. Rousseau, J. M. Friedman, and S. R. Simon, *Proc. Natl. Acad. Sci., U.S.A.*, **76**, 4409 (1979); (b) J. M. Friedman, R. A. Stepnowski, M. Stavola, M. R. Ondrias, and R. Cone, *Biochemistry*, **21**, 2202 (1982); (c) J. Terner, T. G. Spiro, M. Nagumo, M. F. Nicol, and M. A. El-Sayed, *J. Am. Chem. Soc.*, **102**, 3238 (1980).

(5) (a) A. Fulton and L. E. Lyons, *Aust. J. Chem.*, **21**, 873 (1968); (b) A. Nakajima and H. Akamatu, *Bull. Chem. Soc. Jpn.*, **42**, 3030 (1969).

(6) S. A. Alkatis and M. Grätzel, *J. Am. Chem. Soc.*, **98**, 3549 (1976).

(7) (a) G. N. Lewis and D. Lipkin, *J. Am. Chem. Soc.*, **64**, 2801 (1942);

(b) F. T. Taylor and B. C. Saunders, *J. Chem. Soc.*, 3529 (1950); (c) H. Hasegawa, *J. Phys. Chem.*, **65**, 292 (1961); (d) K. Takemoto, H. Matsusaka, S. Nakayama, K. Suzuki, and Y. Ooshika, *Bull. Chem. Soc. Jpn.*, **41**, 764 (1968); (e) B. Kratochvil and D. Zatko, *Anal. Chem.*, **40**, 422 (1968).

(8) R. E. Hester and K. P. J. Williams, *J. Chem. Soc., Faraday Trans. 2*, **77**, 541 (1981).

(9) M. Bridoux and M. Delhaye, *Adv. Infrared Raman Spectrosc.*, **2**, Chapter 4 (1976).

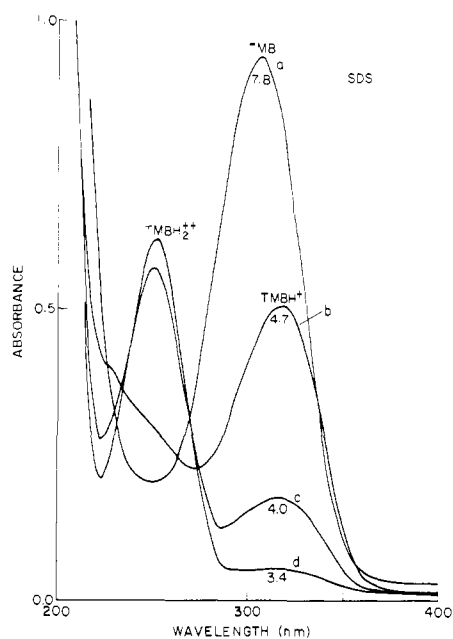


Figure 3. Absorption spectra of TMB in SDS micellar solution as a function of pH.

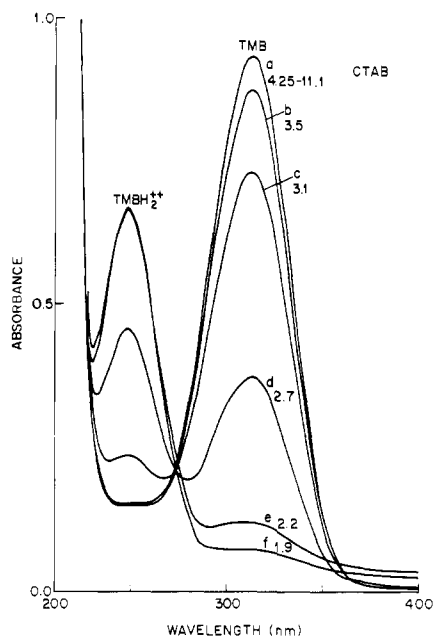
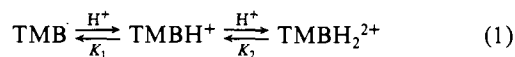


Figure 4. Absorption spectra of TMB in CTAB micellar solution as a function of pH.

different spectra are distinguishable as the pH is lowered from 10.0 to 2.0 in accord with the reactions



TMB has an absorption peak near 300 nm, TMBH⁺ a peak near 310 nm, and TMBH₂²⁺ a peak at 250 nm. pK_a values obtained from these spectra appear in Table I. The value for pK_{a1} is approximate because of overlap of the absorption spectra of TMB and TMBH⁺.

The protonation behavior is strongly affected by dissolving TMB in aqueous ionic micellar solutions. Figure 3 gives the absorption spectra of TMB in SDS as a function of pH. As in MeOH/H₂O solutions, three different forms of TMB exist; the λ_{max} positions show small solvent shifts. The major change in behavior is the increase in the observed pK_a values noted in Table I. SDS solvation has shifted the equilibria toward the protonated forms at a lower hydrogen ion concentration.

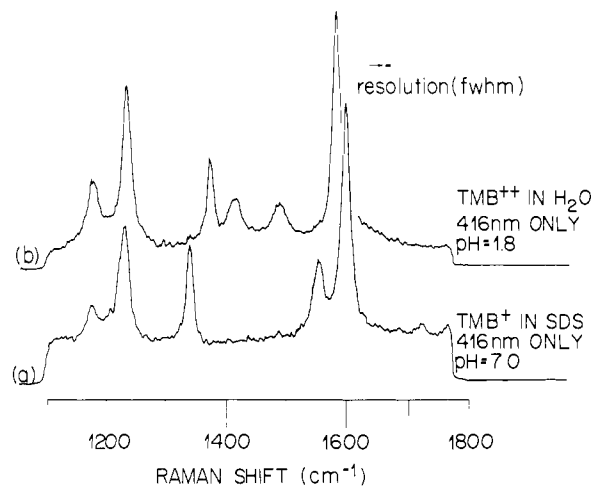


Figure 5. Reference Raman spectra (416 nm): (a) TMB⁺ made in SDS micellar solution by oxidation with dilute Br₂ water; (b) TMB²⁺ formed by oxidation of a TMBH₂²⁺ solution (pH 1.8) with Br₂ water. The instrumental resolution (≈5 cm⁻¹ fwhm) is shown.

Table II. Raman Frequencies (cm⁻¹)

mode type ^a	TMB ⁺	I	TMB ²⁺
ring C-C stretch	1604	1606	1590
781-cm ⁻¹ overtone	1559	1561	1495
inter-ring C-C stretch	1343	1346	1420
C-H in-plane bend	1234	1241	1372
C-H out-of-plane bend	991	991	1239
	941	941	1182
ring breathing	781	781	927
			759
			636

^a Mode type after Hester.⁸

TMB dissolved in CTAB shows yet different behavior. The absorption spectra as a function of pH for this solution is shown in Figure 4. Instead of three states of protonation, TMB in CTAB exhibits only two. These two forms are assigned to unprotonated TMB (λ_{max} 310 nm) and TMBH₂²⁺ (λ_{max} 250 nm) as explained in the Discussion section.

TMB has negligible solubility in pure water at neutral pH. Below pH ≈ 1.8, absorption spectra show TMB dissolves as TMBH₂²⁺. If such a solution is neutralized, TMB precipitates without forming appreciable TMB⁺. We conclude that, in the micellar solutions, any TMB or TMBH⁺ is located in the micellar interior, or on the surface. TMBH₂²⁺ is present principally in the aqueous phase.

2. TMB⁺ and TMB²⁺ Reference Resonance Raman Spectra.

Our ability to generate Raman spectra of transient species at concentrations of 10⁻³ M and below requires use of electronic resonance Raman enhancement, so that the transient Raman signal will be detectable with respect to that of the solvent and other species present. Both TMB⁺ and TMB²⁺ have absorption bands in the blue, and a 416-nm probe laser wavelength generates intense resonance Raman spectra from these species. Figures 2-4 show that the ground electronic states of TMB, TMBH⁺, and TMBH₂²⁺ are essentially transparent at 416 nm; we normally do not detect these species in the presence of TMB⁺ or TMB²⁺.

A 10⁻³ M TMB solution in SDS micelles at neutral pH is optically clear. Treatment with dilute Br₂ water produces an intense green solution whose absorption spectrum matches that reported for TMB⁺ in polar organic solvents.^{6,7} The pulsed 416-nm resonance Raman spectrum obtained from this solution is shown in Figure 5a. This spectrum is essentially the same as that previously reported⁸ and assigned to TMB⁺. The frequencies are given in Table II.

As previously mentioned, in pure water at pH ≈ 1.8, TMB forms the diprotonated species TMBH₂²⁺. Treatment of this solution with bromine water gives an orange solution with a visible absorption spectrum matching that known for TMB₄²⁺.^{7c} Probing

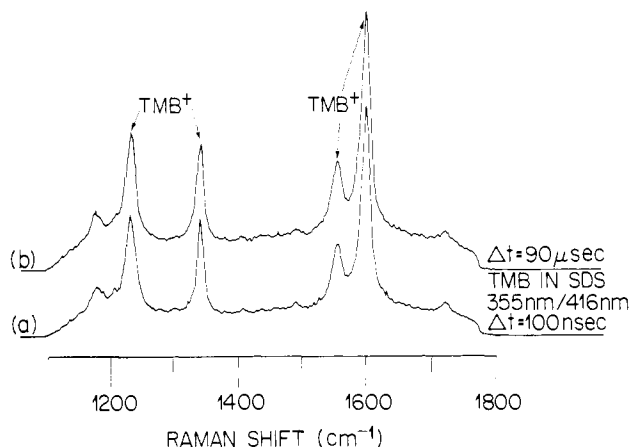
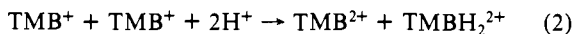


Figure 6. Transient Raman spectra of TMB⁺ in SDS micellar solution: (a) $\Delta t = 0.1 \mu\text{s}$; (b) $\Delta t = 90 \mu\text{s}$.

this solution at 416 nm yields the Figure 5b Raman spectrum, which is assigned to TMB²⁺. The corresponding frequencies are tabulated in Table II.

Table II gives mode assignments for TMB⁺ from Hester and Williams.⁸ Our frequencies are close to theirs with the exception of the in-plane C-H bend (1234 cm⁻¹) which lies 7 cm⁻¹ below their value. They showed that the frequency increase in the C-C inter-ring mode from TMB to TMB⁺ implies a partial quinoid structure as in Figure 1. This mode appears to increase another 29 cm⁻¹ in TMB²⁺, suggesting a greater quinoid contribution as in Figure 1. In TMB²⁺, the decrease in the intra-ring C-C stretch is puzzling.

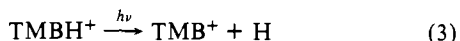
A remaining unresolved question concerns the existence and spectra of the protonated ion TMBH²⁺, which to our knowledge has not been previously reported. TMB⁺ in acidic media undergoes a net disproportionation reaction



whose equilibrium constant lies far to the right-hand side. In the cases of static TMB⁺ in neutral SDS micelles, or in 1:1 H₂O/CH₃OH solution, a lowering of pH yields the two right-hand-side species in absorption spectra. In the resonance Raman spectra, one sees a disappearance of TMB⁺ and a growing in TMB²⁺. At present there is no evidence that, even if TMBH²⁺ is transiently present, its Raman spectrum is detectably different from that of TMB⁺.

3. TMB Transient Resonance Raman Spectra. (A) **H₂O Solvent.** As previously mentioned, TMBH₂²⁺ dissolves in H₂O below pH ≈ 1.8 . Photolysis of a 10⁻⁴ M solution at 266 nm, followed $\Delta t = 100$ ns later by a 416-nm probe pulse, produces an intense resonance Raman spectrum identical with the TMB⁺ spectrum in Figure 5a. This spectrum evolves with time into the TMB²⁺ spectrum, Figure 5b. The transition rate increases with 266-nm photolysis pulse energy; this result suggests a bimolecular reaction as in eq 2. At 266-nm fluence levels of ≈ 0.4 J/cm²-pulse, the transition rate dependence upon energy saturates. This fluence is sufficient to photolyze every molecule in the interaction region. If we assume near saturation, then the rate of TMB²⁺ production implies a bimolecular rate constant of $k_1 \sim 5 \times 10^9$ M⁻¹ s⁻¹.

(B) **Anionic SDS Micellar Solutions.** Figure 6a shows the 416-nm Raman spectrum of a 10⁻³ M solution at pH 7.0, $\Delta t = 100$ ns after a 355-nm pump pulse. The TMB⁺ spectrum is observed, identical with that seen following chemical oxidation in SDS solutions and photoionization in various polar organic solvents. In the pH range where Figure 3 indicates that ground-state TMB is protonated before excitation, exactly the same spectrum is obtained. It may be possible in this pH range that excitation leads to H-atom ejection



thus yielding the TMB⁺ spectrum directly. However, it seems more likely that simple photoionization occurs, implying that we

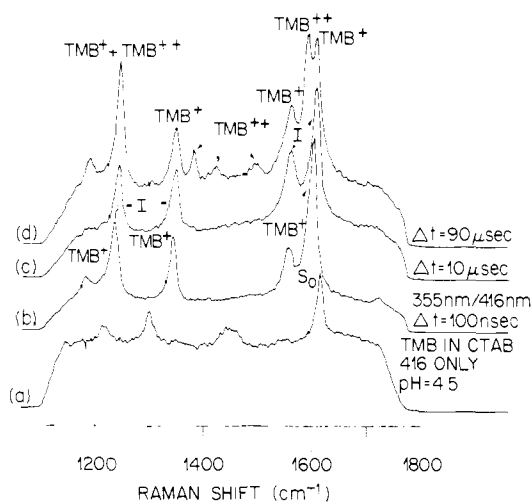


Figure 7. Transient Raman spectra of TMB⁺ and TMB²⁺ in CTAB micellar solutions: (a) without photolysis, showing ground electronic state (S_0) peaks; (b) TMB⁺ initially ($\Delta t = 0.1 \mu\text{s}$) following photoionization; (c) "I" formed from TMB⁺ at $\Delta t = 10 \mu\text{s}$; (d) partial formation of TMB²⁺ at $\Delta t = 90 \mu\text{s}$. Peaks labeled TMB⁺ in this trace actually refer to "I".

observe TMBH²⁺ with the same spectrum as TMB⁺.

There is no time evolution of this spectrum, and the characteristic visible absorption of TMB⁺ remains for days after photolysis. As previously concluded by Alkatis and Grätzel,⁶ TMB⁺ must be especially stabilized inside the SDS micelles by the negative sulfate surface groups.¹⁰ The photoelectron is thermalized in the aqueous phase and prevented from transferring back to TMB⁺ by the static surface potential. Such photolyzed solutions, if brought to low pH, do *not* show the disproportionation reaction 1. The TMB⁺ ions, inside the SDS micelles, apparently cannot approach each other close enough to transfer an electron and disproportionate.¹⁰

(C) **Cationic Micellar Solutions.** An entirely different and interesting behavior occurs in these systems. The 416-nm Raman spectrum without UV excitation of TMB in CTAB at pH 4.5 is shown in Figure 7a. The peak labeled S_0 is a ground-state peak of TMB. The continuous background is due mostly to solvent Raman scattering.

When the probe pulse is preceded 100 ns by a 355-nm pulse, the more intense TMB⁺ spectrum shown in Figure 6b is obtained. This initial spectrum is the same as the TMB⁺ spectrum observed inside the SDS micelle in Figure 6a.¹⁰ However, unlike the SDS case, this spectrum evolves with time as shown in Figure 7c. At $\Delta t = 10 \mu\text{s}$ the lines at 1234 and 1343 cm⁻¹ have shifted to higher frequency, and the intensity ratio between the peaks at 1559 and 1604 cm⁻¹ has increased. We have labeled the species giving rise to this shifted spectrum "I" (see Table II for "I" frequencies). At still longer Δt , a further evolution in the spectrum is observed, as illustrated in Figure 6d, taken at a delay time of 90 μs . Comparison of this spectrum with those in Figure 4 shows the presence of both "I" and TMB²⁺.

For pH < 2.8 the spectra and time evolution observed are the same as previously described for TMBH₂²⁺ in pure water. In this case, TMB is doubly protonated and exits the micelle before excitation. Initially TMB⁺ (TMBH₂²⁺?) is observed with subsequent disproportionation to TMB²⁺. No formation of "I" is observed prior to TMB²⁺ formation.

The behavior of TMB solubilized in other cationic micelles, such as cetyltrimethylammonium chloride (CTAC) and dodecyltrimethylammonium bromide (DTAB), parallels that of TMB in CTAB. At short Δt the characteristic TMB⁺ spectrum is observed followed by evolution into the "I" spectrum and finally observation of the TMB²⁺ spectrum. The "I" spectrum varies slightly with

(10) "Inside" in this context does not imply that TMB⁺ is at the center of the micelle. It simply implies that the molecule is somewhere below the Stern layer of solvated surfactant ionic end groups.

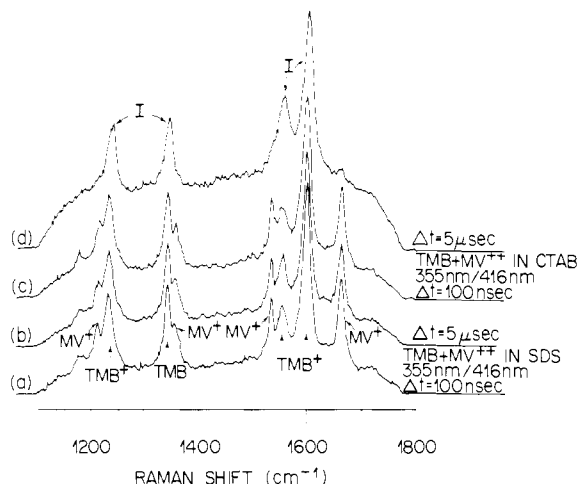


Figure 8. Transient Raman spectra of TMB⁺ and MV⁺ in micellar solutions: (a) SDS, showing TMB⁺ and MV⁺ at $\Delta t = 0.1 \mu\text{s}$; (b) the same solution at $\Delta t = 5 \mu\text{s}$; (c) CTAB, showing TMB⁺ and MV⁺ at $\Delta t = 0.1 \mu\text{s}$; (d) the same solution at $\Delta t = 5 \mu\text{s}$ demonstrating decay of the MV⁺ peaks.

micelle, showing small frequency and intensity shifts from one surfactant to the other.

(D) Reduction of Methylviologen by the Ejected Electron. The organic ion methylviologen (MV²⁺) is soluble in water as the dichloride, has a standard reduction potential $V_0(\text{MV}^{2+}/\text{MV}^+) = -0.44 \text{ V}$ (SHE), and is transparent at both 416 and 355 nm. The reduced form MV⁺ has an intense absorption near 400 nm and exhibits a strong resonance Raman spectrum at 416 nm. MV⁺ can reduce dissolved O₂ at essentially a diffusion-controlled rate.

In a control experiment, a 10⁻³ M MV²⁺ aqueous SDS micellar solution was photolyzed at 355 nm. At $\Delta t = 100 \text{ ns}$, the 416-nm Raman spectrum showed no detectable MV⁺, as expected. Figure 8a shows the corresponding 416-nm spectrum observed following 355-nm photolysis of a neutral pH SDS micellar solution containing 10⁻³ M TMB (inside the micelle) and 10⁻³ M MV²⁺ (in the double layer). This figure shows the normal TMB⁺ spectrum in addition to several new peaks. These new peaks are assignable to MV⁺ by comparison with spectra from chemically reduced MV²⁺ solutions. There is no rise time on the MV⁺ spectra; time resolution is limited to about 50 ns by interfering TMB fluorescence.

Within our resolution, the MV⁺ spectrum is identical with that obtained in simple aqueous solution. Neither the TMB⁺ nor the MV⁺ signal shows decay at $\Delta t = 5 \mu\text{s}$ as shown in Figure 5b. The MV⁺ signal is still present at 90 μs in an O₂-saturated solution.

Figure 8c gives the Raman spectrum at short Δt for a CTAB solution of TMB and MV²⁺. Again both TMB⁺ and MV⁺ are observed, in about the same ratio and absolute yield as was observed in SDS solution. However, now the MV⁺ signal decays completely within 5 μs following UV photolysis, as shown in Figure 8d. This decay is not accompanied by a decrease in the TMB⁺ signal, but can be slowed by elimination of O₂ from the solution. The appearance and decay of the MV⁺ peaks apparently does not affect the evolution of the TMB⁺ spectrum into the "I" spectrum, as observed in Figure 8d.

Discussion

1. TMB Protonation Equilibria. Ionic micelles, depending on the sign of their surface charge, can either stabilize or destabilize charged species in the micelle interior.^{6,11} In addition, [H₃O⁺] at the micelle surface is different from the bulk water owing to

the static potential gradient. The protonation behavior of TMB provides a particularly clear example of these local environmental effects.

pK_a changes in micelle-solubilized indicator dyes have been previously reported.¹² If we neglect free energy changes for the moment, the surface value of the pH (pH_s) at the simplest level of theory,¹³ is

$$pH_s = pH + e\psi/2.3kT \quad (4)$$

where ψ is the static surface potential. For TMB, it is likely that the N(CH₃)₂ group, when it is protonated, is in the Stern layer. While actual potential values are somewhat uncertain, Stigter gives $e\xi/kT = 5.5$ for SDS, where ξ is the electrokinetic potential at the outside of the Stern layer.¹⁴ This value predicts a pH_s increase of 2.5 units, which is close to the observed pK_{a1} change, but somewhat more than the pK_{a2} change, in SDS.

In CTAB, a decrease in pK_{a1} is observed, as expected because here pH_s decreases. However, the decrease is only 1.2 units. This suggests that the changes in free energies are also contributing to this value. The solvation energy of a positive ion inside a CTAB micelle is less than in water (or 1:1 CH₃OH/H₂O).¹⁵ These considerations are qualitative as accurate values for solvation energies and pH_s values are not known. Note that there have been previous attempts to separate solvation and pH_s effects in ionic micelles.¹⁶

Once the TMBH⁺ is formed, it appears to exit the micelle. In the aqueous phase TMBH⁺ is protonated to form TMBH₂²⁺. This appears to be the reason why only two species are observed in the static absorption spectra of TMB in CTAB (Figure 3).

2. TMB⁺ in Ionic Micelles. As previously described, TMB⁺ in anionic SDS micelles is especially stabilized energetically. Its Raman spectrum here is identical with its spectrum in polar organic and acidic aqueous (TMBH₂²⁺?) solvents. The micellar environment inhibits both the electron back-transfer,⁶ and the acidic disproportionation reaction between two TMB⁺s. There is no evidence for TMB⁺ motion following photoionization of TMB.

Kevan and co-workers have recently studied TMB⁺ ESR spectra in frozen and room-temperature SDS micellar solutions. They also conclude that "TMB⁺ has not moved much relative to its precursors TMB."¹⁷

Neutral aromatic TMB apparently dissolves in the hydrocarbon-like micelle interior in both CTAB and SDS micelles. We interpret the fact that the initial TMB⁺ spectrum in CTAB is identical with the SDS spectrum to imply that TMB⁺ is initially created in the micelle interior.¹⁰ A cation in CTAB surrounded by positive alkyl ammonium surface groups is unstable. The anisotropic part of the static surface potential and an increased hydrophilic solvation in water tend to draw TMB⁺ out of the interior. The Raman spectra show a slow, microsecond time scale evolution of the characteristic TMB⁺ spectrum into the "I" spectrum of Figure 4a. We attribute "I" to TMB⁺ on the boundary of the micelle, perhaps with a positively charged end solvated in the Stern layer. TMB⁺ does not permanently exit the micelle as we do not observe again the spectrum characteristic of TMB⁺ in polar organic and acidic aqueous solutions.

In the previously mentioned ESR studies, a TMB⁺ signal could not be observed in room-temperature photolysis of cationic micellar solutions. This is at least consistent with our observation of a TMB⁺ disproportionation reaction. TMB⁺ is observed following 77 K photolysis; here it is likely that the formation of "I" we observe is thermally hindered.

Corroborating evidence for the assignment of "I" comes from the observation that "I" forms in the other cationic micelles studied (DTAB, CTAC), but shows small differences from one micelle

(11) (a) S. A. Alkaitis, G. Beck, and M. Grätzel, *J. Am. Chem. Soc.*, **97**, 5723 (1975); (b) S. A. Alkaitis, M. Grätzel, and A. Henglein, *Ber. Bunsenges. Phys. Chem.*, **79**, 541 (1975); (c) S. M. Beck and L. E. Brus, *J. Chem. Phys.*, **75**, 1031 (1981); (d) S. C. Wallace, M. Grätzel, and J. K. Thomas, *Chem. Phys. Lett.*, **23**, 359 (1973); (e) M. Grätzel and J. K. Thomas, *J. Phys. Chem.*, **78**, 2248 (1974); (f) J. K. Thomas and P. Piciulo, *J. Am. Chem. Soc.*, **100**, 3239 (1978).

(12) P. Pasupati and K. Banerjee, *J. Phys. Chem.*, **68**, 3567 (1967).

(13) J. T. Davies and E. K. Rideal, "Interfacial Phenomena", 2nd ed., Academic Press, New York, 1963, eq 2.53.

(14) D. Stigter, *J. Phys. Chem.*, **83**, 1670 (1979).

(15) L. E. Brus, to be submitted for publication.

(16) M. S. Fernandez and P. Fromherz, *J. Phys. Chem.*, **81**, 1755 (1977).

(17) P. A. Narayana, A. S. W. Li, and L. Kevan, *J. Am. Chem. Soc.*, **103**, 3603 (1981); P. A. Narayana, A. S. W. Li, and L. Kevan, *ibid.*, in press.

to the other. Therefore "I" depends on the exact nature of the micelle and cannot be a bulk-solvated species. The "I" spectrum is only slightly different from the reference TMB⁺ spectrum of Figure 4a, indicating a small geometrical change. Physically, the static field and asymmetric solvating environment in the Stern layer may have the effect of partially localizing the + charge on one N(CH₃)₂ group solvated in water as shown in Figure 1. In the free molecule, the + charge must be symmetrically distributed in the two halves of the molecule. A TMB⁺ molecule, with a N⁺(CH₃)₂ group solvated by H₂O in the Stern layer, is physically similar to a CTAB molecule, which has a N⁺(CH₃)₃ group solvated by H₂O in the Stern layer. "I" may thus correspond to TMB⁺ incorporated into the micelle structure somewhat like at a CTAB molecule.

Further evolution of the spectrum at longer times is observed and can be correlated to the production of TMB²⁺ as in eq 2. The rate of appearance of TMB²⁺, and disappearance of TMB⁺, is dependent on the pump laser power, as expected for a bimolecular process. The observed rate in the near-saturation limit is $k_1 \sim 3 \times 10^7 \text{ M}^{-1} \text{ s}^{-1}$ and is independent of pH in the range 4–10. Reaction 2 is slowed by more than a factor of 100 as compared with water (pH 1.8) because "I" is bound to the micelle. The relative concentration of TMB and micelles are such that only about 50% of the micelles contain a TMB molecule. Therefore, it is likely that the colliding TMB⁺ molecules are from different micelles.

At pH <3 the TMB molecules within the micelle protonate, exit the micelle, and finally solvate in the double layer as TMBH₂²⁺. For this reason "I" is not observed prior to TMB²⁺ appearance at low pH. The reaction sequence is similar to that described in acidic water.

3. Electron Capture by Aqueous MV²⁺. The solvated e⁻ in water is able to reduce MV²⁺. In both SDS and CTAB micelles, the photoionization yields are of similar magnitude and unaffected by the presence of MV²⁺ in solution at our rather high fluence levels. In the absence of MV²⁺, the solvated e⁻ in water is formed. To our knowledge there is no estimate on the distance that the solvated e⁻ will form from its originating micelle. In the SDS case there is a strong increase in MV²⁺ concentration in the micellar double layer,¹⁸ while in the CTAB case a depletion occurs. We do not observe a strong difference in MV⁺ yield in the two cases, which appears to imply that, on our time scale, all e⁻ have reacted with MV²⁺. The solvated e⁻ may be an intermediate species in the CTAB case. Further experiments at low MV²⁺ concentrations would be interesting.

Unfortunately, and unlike the case of "I" formation with TMB⁺, the MV⁺ Raman spectra do not suggest any subsequent change of environment. In this regard, however, the decay kinetics of MV⁺ are interesting. In a homogeneous water solution with [O₂] $\sim 3 \times 10^{-4} \text{ M}$, MV⁺ lives for $\approx 1 \mu\text{s}$ before reducing O₂. In SDS solution MV⁺ lives for at least 90 μs , even in an O₂ saturated solution. MV⁺ is "protected" from reaction with O₂. It is well documented, using O₂ quenching of excited-state luminescence, that species dissolved in micelle interiors are partially protected from reaction with oxygen.¹⁹ In an O₂-saturated solution the O₂ entry rate into a micelle is $\sim 2 \times 10^7 \text{ s}^{-1}$, and the diffusional time to collide with MV⁺ inside the micelle would be $\sim 20\text{--}100 \text{ ns}$.^{19d} Thus in SDS any oxidation by O₂ occurs at a rate far below

diffusion controlled. It may be that this reaction, which yields ionic products, is endothermic in a hydrocarbon environment.

Although MV²⁺ easily dissolves in pure water, in SDS micellar solutions it is strongly associated with the micelles¹⁸ and is at or near the micelle surface in the aqueous double layer. Upon being reduced to MV⁺, the hydrophobic character will increase and MV⁺ might move "inside" the micelle. The long MV⁺ lifetime observed suggests this species is sufficiently inside the micelle to be protected from O₂.

As previously discussed, it is less likely that MV⁺ will be preferentially stabilized inside a cationic CTAB micelle. Our shorter MV⁺ lifetime here, dependent upon [O₂], suggests MV⁺ remains in the aqueous phase in this case. Obviously the hydrophobic character of MV⁺ can be further increased if a long alkyl chain is attached. It is interesting to note that Grätzel and co-workers report that such a reduced species (C₁₂MV⁺), if formed in the aqueous phase, moves inside CTAC micelles at a near-diffusion-controlled rate.²⁰

Final Remarks

We have attempted to use transient Raman spectroscopy to detect motion of chemical species from one environment to another, via subtle changes in the Raman spectra, with partial success. In the case of TMB⁺ forming "I", we observe peak shifts of 3–7 cm⁻¹ coupled with relative intensity changes. Yet possibly in the case of MV⁺ in various environments, and in the case of TMB⁺ entirely inside and entirely outside of the micelle, no change is currently detectable.

Our present resolution is about 5 cm⁻¹ (fwhm). At higher resolution there could yet be reproducible differences among these spectra. Quantification of line shapes might bring out such differences. In spontaneous Raman spectroscopy, the line shape is typically inhomogeneous²¹ and on the order of 10–15 cm⁻¹. Higher order Raman spectroscopies, such as CSRS and CARS, have different line shapes: it may be that one of these methods could also be useful in detecting environmental differences.

Conclusions

- (1) In SDS and CTAB micelles, the TMB protonation equilibria shift in the directions expected from the surface pH changes.
- (2) In SDS micelles, TMB⁺ produced by photoionization of TMB inside the micelle is stable. Electron back-transfer and ion bimolecular reactions are prevented by encapsulation inside the micelle.
- (3) In CTAB micelles, the resonance Raman spectrum of TMB⁺ initially inside the micelle evolves into an intermediate spectrum, thought to represent a slightly distorted TMB⁺ *asymmetrically* solvated in the Stern layer. This TMB⁺ species undergoes a bimolecular disproportionation reaction, although at a rate orders of magnitude slower than that observed in homogeneous acidic solution.
- (4) In CTAB micellar solutions, the ejected electron can reduce MV²⁺ in the aqueous phase. MV⁺ subsequently decays by reducing dissolved O₂. In SDS micellar solutions MV⁺ is protected from oxidation by O₂, perhaps by moving inside the SDS micelles.

Acknowledgment. We enjoyed discussions of these experiments with L. Kevan and A. Warshel.

Registry No. TMB, 366-29-0; TMB⁺, 21296-82-2; TMB²⁺, 2655-65-4; TMBH₂²⁺, 46902-94-7; TMBH⁺, 46902-93-6; SDS, 151-21-3; CTAB, 57-09-0; MV²⁺, 1910-42-5; O₂, 7782-44-7; MV⁺, 79028-21-0.

(18) (a) M. A. J. Rodgers and J. C. Becker, *J. Phys. Chem.*, **84**, 2762 (1980); (b) R. H. Schmehl and D. G. Whitten, *J. Am. Chem. Soc.*, **102**, 1938 (1980).

(19) (a) M. Grätzel and J. K. Thomas, *J. Am. Chem. Soc.*, **95**, 6885 (1973); (b) M. W. Geiger and N. J. Turro, *Photochem. Photobiol.*, **22**, 273 (1975); (c) A. A. Gorman, G. Lovering, and M. A. J. Rodgers, *ibid.*, **23**, 399 (1976); (d) N. J. Turro, M. Aikawa, and A. Yekta, *Chem. Phys. Lett.*, **64**, 473 (1979).

(20) P. A. Brugger, P. P. Infelta, A. M. Braun, and M. Grätzel, *J. Am. Chem. Soc.*, **103**, 320 (1981).

(21) S. M. George, H. Auweter, and C. B. Harris, *J. Chem. Phys.*, **73**, 5573 (1980).